



Cite this: *Energy Environ. Sci.*, 2022, 15, 786

CO₂ capture by pumping surface acidity to the deep ocean†

Michael D. Tyka, * Christopher Van Arsdale and John C. Platt

To remain below 2 °C of warming, most IPCC pathways call for active CO₂ removal (CDR). On geological timescales, ocean uptake regulates atmospheric CO₂ concentration, with two homeostats driving CO₂ uptake: dissolution of deep ocean carbonate deposits (1 ka timescales) and terrestrial weathering of silicate rocks (100 ka timescales). Many current ocean-based CDR proposals effectively act to accelerate the latter. Here we present a method which relies purely on the redistribution and dilution of acidity from a thin layer of the surface ocean to a thicker layer of deep ocean, in order to reduce surface acidification and accelerate carbonate homeostasis. This downward transport could be seen analogous to the action of the natural biological carbon pump. The method offers advantages over other ocean alkalinity and CO₂-stripping methods: the conveyance of mass is minimized (acidity is pumped *in situ* to depth), and expensive mining, grinding and distribution of alkaline material is eliminated. No dilute substance needs to be concentrated, reducing the quantity of seawater to be processed. Finally, no terrestrial material is added to the ocean, avoiding significant alteration of seawater ion concentrations or issues with heavy metal toxicity (encountered in mineral-based alkalinity schemes). The artificial transport of acidity accelerates the natural deep ocean compensation by calcium carbonate. It has been estimated that the total compensation capacity of the ocean is on the order of 1500 GtC. We show through simulation that pumping of ocean acidity could remove up to 150 GtC from the atmosphere by 2100 without excessive increase of local pH. The permanence of the CO₂ storage depends on the depth of acid pumping. At >3000 m, ~85% is retained for at least 300 years, and >50% for at least 2000 years. Shallow pumping (<2000 m) offers more of a stop-gap deferral of emissions for a few hundred years. Uptake efficiency and residence time also vary with the location of acidity pumping. Requiring only local resources (ocean water and energy), this method could be uniquely suited to utilize otherwise-unusable open ocean energy sources at scale. We present a brief techno-economic estimate of 130–250\$ per tCO₂ at current prices and as low as 93\$ per tCO₂ under modest learning-curve assumptions.

Received 21st May 2021,
Accepted 24th December 2021

DOI: 10.1039/d1ee01532j

rsc.li/ees

Broader context

In addition to near-total decarbonization of the world economy it is increasingly clear that already emitted CO₂ will also need to be actively removed from the atmosphere in order to stabilize the Earth's temperature. Due to their natural role in regulating CO₂ over geological periods of time, the weathering of alkaline minerals and the subsequent flow of alkalinity into the oceans are an attractive candidate for CO₂ sequestration with the potential to store many hundreds of gigatonnes of CO₂. With the aim of accelerating such dissolution most prior work has focused on terrestrial minerals, while less attention has been paid to the alkaline carbonate sediments in the deep ocean. Our electrochemical approach of pumping surface acidity into deeper ocean layers could provide a means to induce the dissolution of alkaline mineral deposits (calcite) in the deep ocean while accelerating CO₂ uptake at the surface. The approach is uniquely suited for open ocean energy sources since no terrestrial material is needed and could thus provide an interesting new technology in the overall portfolio of negative emissions that will be needed in the latter half of this century.

1 Introduction

Stabilizing the earth's climate into the next centuries will require a near total decarbonization of the world energy supply, *i.e.* reducing emissions from their current peak levels. However,

some industrial processes, such as industrial heat and concrete manufacturing as well as emissions from land use changes, air travel, or livestock are very difficult to decarbonize.¹ Further, even if future emissions were curbed, enough historical CO₂ has already accumulated in the atmosphere to cause problematic warming and could trigger tipping points. Thus, the vast majority of IPCC RCP2.6 scenarios which remain under 2 °C of warming require negative emissions on the order of 150 GtC before 2100^{2,3} in addition to rapid decarbonization. On geological timescales

Google Inc., 601 N 34th St, Seattle, WA 98103, USA. E-mail: mike.tyka@gmail.com

† Electronic supplementary information (ESI) available. See DOI: 10.1039/d1ee01532j

several mechanisms act to regulate the atmospheric CO₂ concentration: over periods of hundreds of years the oceans will absorb the majority of the excess CO₂ leading to very significant surface acidification.⁴ Subsequent downward transport of the CO₂ brings the acidity in contact with CaCO₃ deposits, dissolving them and releasing alkalinity, and thus stabilizing the pH.⁵ On even longer timescales (100 ka), weathering of terrestrial silicate rocks releases new alkalinity to the oceans and allows the previously dissolved CaCO₃ to be redeposited while the lysoclines return to their original depths. The consecutive transfer of the excess CO₂ along these three sinks acts to keep the temperature of the earth within relatively stable bounds over long periods of time.^{6,7} Unfortunately, the response time of even the first of these two buffers is too slow to keep up with the rate of human emissions,^{8,9} leading to a temporary but dangerous spike in atmospheric CO₂ concentrations, warming and surface ocean acidification.

The primary limiting step is the net transport of CO₂ into the deep ocean due to the action of the biological pumps.^{9,10} Anthropogenic CO₂ has not yet penetrated deeply into the ocean, because most of the remineralization of sinking organic matter occurs in the first 500 m beyond the euphotic zone, with peak acidification at about 250 m depth.⁴ Anthropogenic CO₂ has acidified mostly surface waters, impacting carbonate-shell-forming organisms, while staying out of reach of inorganic CaCO₃ deposits located well below the euphotic zone.¹¹ Positive feedbacks are also present in this system, where CO₂-saturated surface waters oppose further CO₂ uptake, reduce the ocean buffering ability and accelerate future pH changes due to the nonlinearity of the carbonate system¹²; these issues are further compounded under increasing stratification and a weakened biological pump predicted for a warming ocean.

While many methods have been proposed to accelerate terrestrial mineral weathering,^{2,13} by mechanical^{14,15} or electrochemical means,^{16,17} accelerating dissolution of sedimentary carbonate minerals has not yet been explored. Here, we examine the feasibility of artificially transporting acidity to the deep ocean, in order to accelerate both the natural carbonate compensation mechanism and the ensuing flux of carbon from the atmospheric reservoir into the ocean (bi)carbonate reservoir. Such an action cannot replace the need for total decarbonization of the economy, but could contribute to blunt the ecological impact of past emissions by dilution in spatial and temporal dimensions. The inventory of erodible CaCO₃ on the ocean floor is estimated to be ~1600 GtC,⁸ theoretically more than sufficient to compensate for the ~640 GtC that humanity has released since preindustrial times.

1.1 Accelerating deep water equilibration

We envision a method to artificially increase the downward transport of acidity from the surface ocean to the deep ocean that first involves electrochemically splitting seawater into acid and base. The weakly alkaline effluent would be released at the surface, while the weakly acidic water would be pumped into the deep ocean (see Fig. 1). In the surface water the alkalinity would thus be raised and the pH stabilized. This maintains an increased flux of CO₂ into the ocean and reduces atmospheric CO₂, helping to alleviate immediate radiative forcing. The

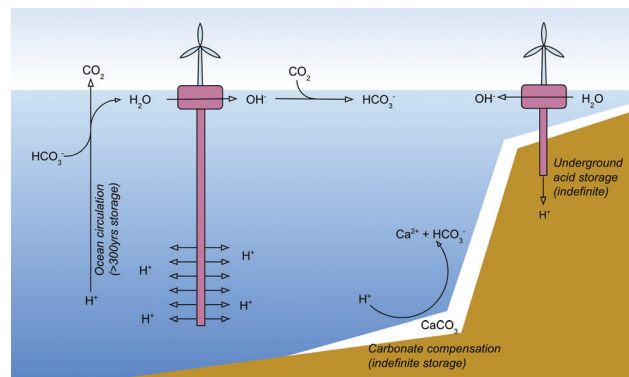


Fig. 1 Schematic showing how pumping of acidity from surface water would accelerate the natural weathering of sedimentary carbonates on the ocean floor and help stabilize atmospheric CO₂. Any acidity that doesn't react with carbonate sediments will eventually return with ocean circulation. Alternatively, for shallow ocean areas, acidity could be pumped into underground formations or depleted oil reservoirs, similar to CCS, leading to permanent CO₂ drawdown into the ocean. Note that for purposes of clarity we represent acidified and basified ocean water as H⁺ and OH⁻, with the respective counter ions, Cl⁻ and Na⁺, not shown explicitly.

increased pH (decreased acidity) would also help stabilize the health of coral reefs¹⁸⁻²⁰ and Coccolithophores and help preserve these ecosystems past the anthropogenic CO₂ spike. Synthesis and subsequent sinking of coccoliths plays a vital role in ballast formation in the biological pump and indirectly aids the downward transport of organic carbon in the ocean²¹. These surface-ocean effects would be the same as those of ocean liming proposals¹³, *i.e.* surface dissolved inorganic carbon (DIC) would increase together with an equally increased alkalinity and the carbonate equilibrium would remain stable. A common approximation¹⁰ for the concentration of carbonate ions is $[\text{CO}_3^{2-}] \approx \text{Alk} - \text{DIC}$, which makes this immediately apparent. Meanwhile the acidic, low-pH effluent could be diluted across a large section of the deep water column using perforated, flexible, deep vertical pipes. As the deep water column contains much more water than the thin surface water layer that the acidity originated in, such redistribution of surface-ocean acidity dilutes the surface acidity and its ecological effects. Isopycnal deep water circulation would then spread and dilute this acidity horizontally, bringing it in contact with calcite sediments. The precise impact of such a redistribution on pH and calcite saturation is complex and will be explored through ocean simulation in this paper.

Comparison with mineral alkalization

A great variety of methods have been proposed to increase ocean capacity for CO₂, without raising ocean acidity, by dissolving terrestrial minerals.¹³ These proposals aim to accelerate the total terrestrial weathering rate and subsequent ocean influx by 1–2 orders of magnitude.² In practice, the mining, grinding, transport and distribution of gigatonnes of rock per year poses significant challenges. If the material is ground to ~100 µm, the dissolution of these minerals is on the order of many decades^{14,15} and particles would sink out of the



mixed layer long before dissolution,²² limiting applicability to shallow coastal areas.²³ Grinding down to 1 μm would enable open ocean distribution, but significantly increase grinding energy costs.²⁴ Iron, abundant in most olivine minerals, would inadvertently fertilize the ocean leading to significant ecological disruption^{2,14} and changes in silicate concentration would shift the phytoplankton species composition towards diatoms.²² Nickel, also found in olivines,^{25,26} is biologically both an essential co-factor and toxic at high concentration with different concentrations optimal for different marine species.²⁷ Chromium is present in flood-basalts and ultra-basic rocks in similar quantities to nickel.²⁵

This proposal shares many properties with the above ocean alkalinity enhancement proposals, with some advantages. Firstly there is no need for large mass transport of alkaline rocks to the ocean¹³ or transport of products away from electrolyzers.²⁸ The only matter transport needed is the pumping of a small amount of water a few kilometers downwards. This locality makes the method uniquely suitable for open ocean deployment and provides a way to use otherwise unusable renewable energy resources. Open waters offer greater scalability at reduced ecological impact as dilution over large areas is trivial. The proposed method also avoids the severe impacts of creating a gigatonne-scale mining operation on terrestrial ecosystems. The net cation composition of the ocean is not changed, avoiding introduction of iron, silicate or toxic trace metals into ocean ecosystems, a major concern with most mineral-based alkalinization approaches.² The redistribution of alkalinity dilutes the already occurring anthropogenic acidification of the surface ocean into the deeper ocean. Due to these advantageous ecological properties, the proposed method may find it easier to gain social license, as it aims to mitigate human impact by spatial and temporal dilution. In general, all ocean alkalinity methods are currently regulated by international maritime laws such as the London Convention²⁹ which would have to be reviewed and possibly amended before deployment could begin at scale.³⁰

We note also that widely discussed biological ocean CDRs³¹ which propose increasing primary biological productivity and sinking of biological matter, such as ocean fertilization, could be seen as equivalent to the acidity pumping proposed here. This is because the vast majority of sunk soft tissue is remineralized in the water column or on the ocean floor, thus acidifying deep waters.³² Only 0.4% of the originally fixed carbon is buried in sediments and permanently removed from circulation.¹⁰ Thus efforts increasing primary biological production likewise rely on the dissolution of deep CaCO_3 deposits to prevent the transported carbon from being re-emitted to the atmosphere on the timescales of ocean circulation. Thus, these methods also ultimately aim to accelerate deep carbonate dissolution, albeit indirectly. The same can be said for efforts to directly inject CO_2 into the deep sea, as the resulting CO_2 lakes or hydrates gradually dissolve.³³

In this paper we present ocean circulation simulations to examine the effects and limitations of large-scale acidity pumping as well as techno-economic arguments which suggest that the cost per tonne of CO_2 could potentially be competitive

with terrestrial direct air capture (DAC) and other negative emissions technologies while avoiding the ecological impacts of accelerated mineral weathering.²

2 Methods

2.1 Global circulation model of acid-base pumping

To simulate the effect of acid-base pumping on surface and deep water pH, as well as net ocean CO_2 uptake, and evaluate the return time of acidity, we used a full ocean circulation model in a 128×64 worldwide spherical polar grid using MITgcm.³⁴ The simulation had cell sizes of $2.8^\circ \times 2.8^\circ$ divided into 20 exponentially spaced depth levels, from 10 m thick at the surface to 690 m thick at depth. The simulation was initialized and forced as detailed in Dutkiewicz *et al.* (2005).³⁵ The MITgcm GEOM and DIC modules were used to simulate the soft tissue and carbonate pumps, as well as ocean-atmosphere gas exchange. A number of studies^{36,37} have simulated addition of alkalinity to the ocean in the context of realistic emission scenarios with increasing atmospheric $p\text{CO}_2$. Here we chose to focus instead on the efficiency of CO_2 uptake and the circulation aspects of acidity return, and thus the atmospheric concentration of CO_2 was simply held constant at 415 ppm similar to work by Köhler *et al.*²²

2.1.1 Perturbation. Custom code was added to simulate the transport of alkalinity from a parameterizable slab of deep water to the top 10 m of surface water corresponding to the pumping of acidity in the opposite direction, keeping the total ocean alkalinity constant. To investigate the fate of alkalinity and acidity separately, some simulations were modified to only alkalize, in which case the total alkalinity change was not conservative. These simulations represent an idealized addition of pure alkalinity to the surface ocean. In all experiments the pumped alkalinity was released into the top 10 m slab (the top most gridcell). The acid-injection slab was approximately 1100 m thick to within the precision allowed by the vertical grid spacing. However, its depth, as well as the lat-lng distribution of pumping, were varied from experiment to experiment, as detailed in the Results section. The movement of volume was not explicitly modelled, as the involved quantities are tiny ($\sim 5 \times 10^{-3}$ Sv GtC^{-1}) compared to the natural ocean overturning circulation.

2.1.2 Carbonate compensation. The return of the acidity with the overturning circulation is the timeframe in which the transported acidity can be neutralized by dissolving carbonate sediments. Both the dissolution of existing CaCO_3 deposit inventories (estimated⁶ at a total of 1600 GtC), and reduction of new carbonate deposition (estimated at 0.27 GtC per year to 0.1 GtC per year^{38,39}) increase net alkalinity in the ocean and would act to neutralize any pumped acidity. Due to the relatively short amount of time that sinking particles spend in the water column, most of the dissolution below the carbonate saturation horizon (CSD) occurs on the ocean floors. Despite the relatively uncertain current carbonate dissolution rates (0.3 GtC per year $\pm 60\%$)¹¹ a basic model of increased carbonate



compensation due to pumped acidity can be constructed. The rate r of seafloor dissolution has been expressed^{40,41} as

$$r = k^*([CO_3^{2-}]_{\text{sat}} - [CO_3^{2-}]) \quad (1)$$

The effective rate constant, k^* , is limited by sediment-side mass transport (K_s) or water-side diffusion (β) through a boundary layer, whichever is slower:^{40,41}

$$k^* = K_s \beta / (K_s + \beta) \quad (2)$$

Most locations of significant (>20%) carbonate content are limited by water-side diffusion,¹¹ as bottom water speeds are relatively slow. Thus the resulting kinetics are linear with respect to the carbonate ion concentration and relatively independent of sediment $CaCO_3$ content. To simulate the dissolution of $CaCO_3$ deposits during our simulations, a gridded map of dissolution rate constant, k^* and sedimentary $CaCO_3$ content was obtained from work by Sulpis *et al.*¹¹ The bottom dissolution rate was then calculated by eqn (1) for all grid tiles where the $CaCO_3$ fraction >10%. For grid tiles containing less than 10% the dissolution rate was set to 0. At the same time, any biological carbonate flux reaching the ocean floor was modelled to have settled onto the seafloor. At steady state the rate of sedimentation and dissolution was found to be relatively balanced, *i.e.* the total ocean alkalinity was not changing rapidly. Riverine alkalinity input was not modelled. An initial simulation allowed the ocean system to equilibrate for 2500 years and was used as the starting point for

all subsequent pumping simulations. All the simulation setups, code modifications and parameters are available.⁴²

3 Results

3.1 Uniform pumping

In our initial simulations alkalinity was pumped uniformly over the entire ocean, wherever the respective depth was available to pump acidity to. The amount of alkalinity pumped was 0.25 Pmol per year, the equivalent to a maximum uptake of 3 GtCeq per year, roughly the same amount as was used by Köhler *et al.*²² Note that throughout this paper we will use units of 1 GtCeq = 0.833 Tmol to provide a better intuitive sense for the quantities involved (relative to human emissions of ~10 GtC per year). Pumping proceeded for 50 years which would yield roughly the required amount of negative emissions called for by most RCP2.6 pathways.

We also investigated lower and higher pumping rates up to 10 GtCeq per year to examine the effect on pH and carbonate saturation and to provide context for assessing a reasonable level of alkalization without excessively affecting marine ecology. Previous work³⁷ examined alkalinity addition as high as ~22 GtCeq per year although such a high rate may not be practical or ecologically safe. After the 50 year pumping period was over the simulation was allowed to continue up to the 5000 year mark to investigate carbonate compensation and the longevity of the stored carbon. To identify the role of carbonate compensation a control run was performed with sediment

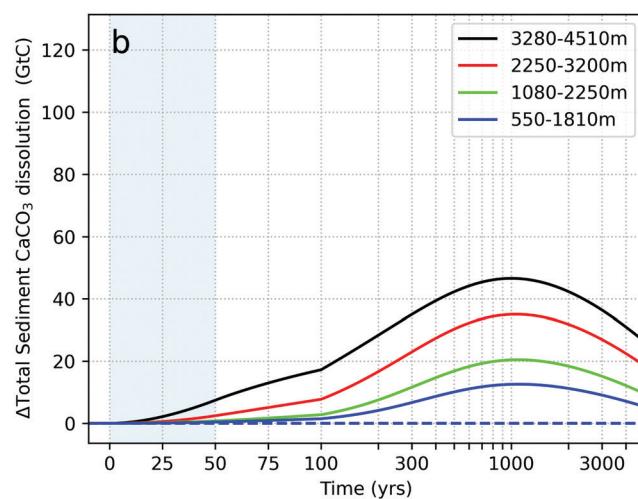
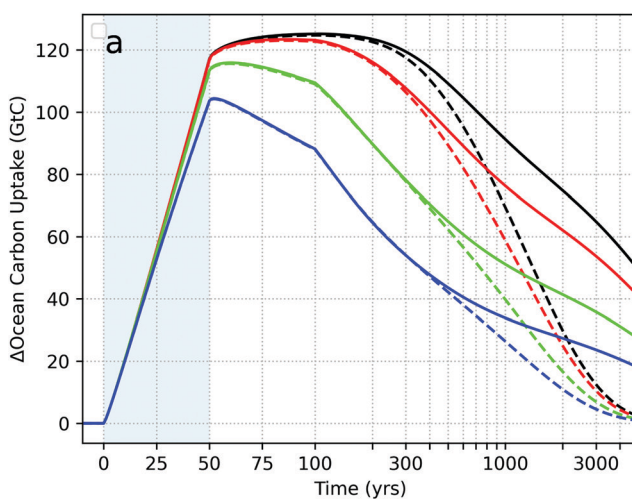


Fig. 2 Shown is the total excess CO_2 uptake and total excess calcite dissolution at the seafloor with respect to time (logarithmic scale past the 100 year mark). Alkalinity and acidity are separated and acidity is pumped to depth, wherever possible, with a total rate of 3 GtC equivalent per year. Different colors represent different depths at which acidity was injected. The solid lines represent simulations including carbonate compensation, whereas the dashed lines are simulations ignoring carbonate compensation. The grey shading indicates the period for which pumping was active (the first 50 years). (a) Shows the total excess carbon (in GtC) absorbed by the ocean due to alkalinity pumping, relative to a reference simulation without any perturbation. Note that the maximal CO_2 uptake reaches ~85% of the total amount of alkalinity moved (150 GtCeq over 50 years), in agreement with the compensation behavior of the carbonate system shown in Fig. S0 (ESI†) (see also Renforth *et al.*¹³). As long as acidity is moved below 2000 m, even in the absence of carbonate compensation, the absorbed carbon is retained well beyond 300 years. (b) Shows the relative increase in global sedimentary carbonate dissolution. When acidity is transported below 3280 m about 40% of the absorbed CO_2 is compensated by calcite. Note that the total excess dissolved calcite begins to drop again at ~1000 years. This is due to the fact that our simulation kept the atmospheric CO_2 concentration constant at 418 ppm, and thus the system begins to return to an equilibrium point where sedimentation rate and dissolution rate balance. The true long-term equilibrium point of the carbonate homeostat will depend strongly on future anthropogenic CO_2 emissions, which are highly uncertain.



compensation turned off. A positive control run was also performed to compare to the case where alkalinity is added at the surface but no compensating acid is deposited at depth, effectively simulating the addition of a fast dissolving alkaline material.

Fig. 2a shows that alkalinity pumping results in rapid uptake of CO_2 , virtually indistinguishable from simple net alkalinity addition to the surface for the first 50 years. In the subsequent period, the depth of acid release strongly determines the return time and the eventual re-emission of any previously captured CO_2 . Injection of acidity in too shallow waters causes reemission within a few hundred years, an insufficient amount of time for any significant amount of carbonate compensation to occur. However, for acid depths greater than 3200 m the CO_2 absorbed does not begin to be re-emitted for at least 300 years, retaining 85–95% of the absorbed CO_2 . For an acidity release below 2250 m, the relaxation half-life of CO_2 return to the atmosphere is found to be ~ 2000 years. This time provides sufficient contact time for deep carbonate dissolution to occur as shown in Fig. 2b, with the global calcite dissolution rate increasing by as much as 0.25 GtCeq per year. We note that the system relaxation time is significantly increased due to this dissolution, as the half life for CO_2 return in the reference simulations without carbonate dissolution was much shorter (~ 1000 years), depending solely on ocean circulation. We note that because carbonate compensation is a bidirectional homeostat, simply balancing net dissolution with net deposition, the proportion of CO_2 which will be permanently removed depends on the future emissions scenarios and the eventual equilibrium point of the ocean. The method proposed here simply allows the homeostat to respond much more quickly than it would have otherwise done.

Fig. 3 tracks median and 95%ile changes in surface and ocean floor pH. See Fig. S1 (ESI[†]) for the corresponding change in calcite saturation. The median surface ΔpH rises rapidly for the first 1–2 years (0.03 per year) but slows within 10 years to a steady rate of 2×10^{-4} per year, reaching a maximum median ΔpH of 0.022 after 50 years. The increased rate of CO_2 dissolution is mostly able to buffer the increase in surface alkalinity. The seafloor pH however continues to decrease throughout the pumping period due to the considerably slower calcite dissolution rate. Despite this, the perturbation is at most -0.15 pH units at its most extreme point. Varying the global pumping rate between 0.3 and 10 GtCeq per year we found a roughly linear dependence of pH and Omega perturbation and pumping rate (Fig. 4). The sensitivity of benthic ecosystems to pH perturbation is poorly understood and requires further research. However, seasonal changes in open-ocean pH can be up to 0.2 pH units⁴³ while diurnal changes in coastal areas can reach as much as a full pH unit.⁴⁴ Using this as a guide we suggest that alkalinity pumping at global rates of 1–3 GtCeq per year may be feasible without excessive stress on marine systems, though this is a critical area in need of further research.⁴⁵

3.2 Location dependence

Uniform pumping is neither practical nor efficient. From a practical perspective, the location of pumping will depend strongly on the mode of deployment (see Discussion). From an oceanographic perspective, both the efficiency of alkalinity

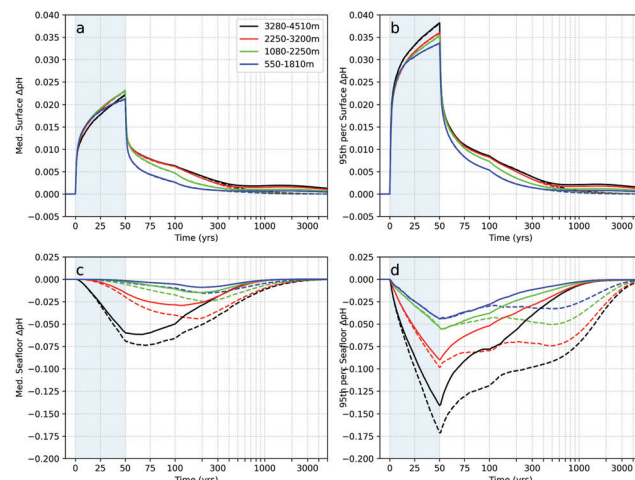


Fig. 3 Median and 95%ile changes in pH at the surface (a and b) (increase in pH) and at the seafloor (c and d) (decrease in pH) for the same runs. It can be seen that even in locations of most extreme pH change, the localized pH changes are not excessive. The changes at the surface are smaller than at depth (despite originating in a much thinner slice of water) because the lowered partial pressure of CO_2 immediately pulls in more carbon due to the relatively fast equilibration time. At depth the compensation with carbonate deposits proceeds much more slowly and therefore the pH response to acidity pumping is larger over time. Fig. S1 (ESI[†]) shows the equivalent plots of median and 95%ile changes in calcite saturation (Ω).

compensation at the surface and the timescales of return of acidity from deep waters vary substantially depending on the location in the ocean. The former varies due to differences in the uptake efficiency factor and surface currents, while the

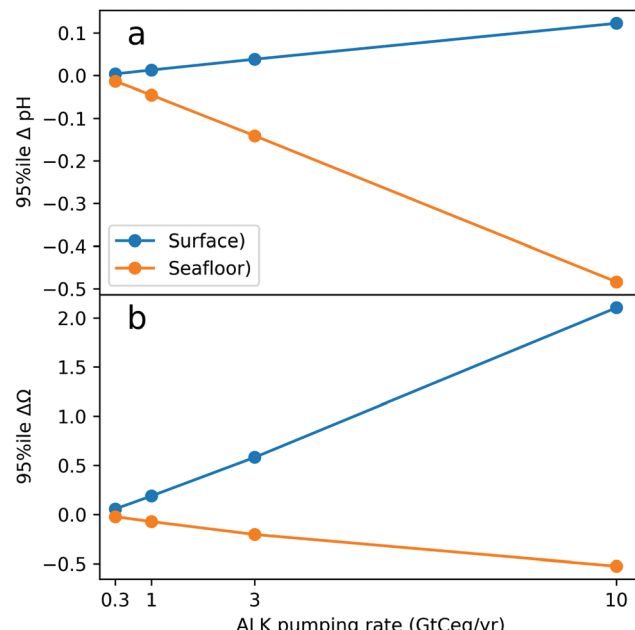


Fig. 4 (a) 95%ile pH changes at the end of 50 year alkalinity pumping across surface and across ocean seafloor for uniform alkalinity pumping at different global rates. (b) Likewise, median changes in calcite saturation (Ω), relative to reference simulation. A roughly linear dependence with respect to alkalinity pumping rate is observed.



latter depends on how soon deep waters are returned to the surface with the global overturning circulation.

The carbonate equilibrium in seawater responds to an increase in alkalinity by shifting towards the carbonate ion. The concomitant reduction in the partial pressure $p\text{CO}_2$ causes an uptake of CO_2 from the atmosphere until equilibrium is restored. The number of moles of CO_2 absorbed for every mole of alkalinity added, the uptake efficiency η_{CO_2} , can be expressed as the ratio of the partial pressure sensitivities of $p\text{CO}_2$ with respect to total alkalinity (Alk) and total inorganic carbon (DIC).^{13,38} This compensation ratio presents a fundamental inefficiency that needs to be taken into account when calculating potential CO_2 uptake of any ocean alkalization method in addition to any process inefficiencies. The commonly used approximations $\text{DIC} \approx [\text{HCO}_3^-] + [\text{CO}_3^{2-}]$ and $\text{Alk} \approx [\text{HCO}_3^-] + 2[\text{CO}_3^{2-}]$ at typical ocean pH yield a good approximation for the uptake factor: (derivation in ESI†).

$$\eta_{\text{CO}_2} = -\frac{\partial p\text{CO}_2}{\partial \text{Alk}} / \frac{\partial p\text{CO}_2}{\partial \text{DIC}} \approx \frac{1}{3 - 2\text{DIC}/\text{Alk}} = \frac{1}{1 + 2[\text{CO}_3^{2-}]/\text{Alk}} \quad (3)$$

which evaluates to ~ 0.8 at average surface ocean concentrations of $\text{DIC} = 2000 \mu\text{M}$ and $\text{Alk} = 2300 \mu\text{M}$. The intuition why η_{CO_2} is smaller than 1 is that while each mole of additionally absorbed CO_2 will be neutralized by one mole of OH^- to bicarbonate, some fraction of it will consume additional OH^- to become a carbonate ion. A full carbonate model^{46,47} was used to calculate the plot in Fig. S1 (ESI†), showing that this uptake factor varies substantially depending on the latitude and is one aspect to determine optimal alkalinity release locations. Alkalinity addition to areas with high efficiency factor will cause a greater uptake of

CO_2 in the near term, however ocean surface currents will tend to move the uptake towards an average efficiency over time, so longer term efficiency can only be predicted with explicit circulation simulation.^{36,37} Furthermore, in our case, the return time of the acidity is dependent on the direction and speed of bottom currents and the proximity to upwelling areas.

We thus performed a grid scan of the ocean, where in each simulation an amount of 100 Tmol per year of alkalinity (0.12 GtCe_{eq} per year) was pumped at any one grid point only. Altogether ~ 1000 independent simulations were conducted, one for every gridpoint with sufficient depth to inject acidity. In each case the entire ocean biogeochemistry was monitored compared to a reference simulation with no pumping.

Fig. 5 and Fig. S3 (ESI†) show the normalized total uptake of CO_2 , such that a value of 1.0 represents an ocean uptake equimolar to the amount of alkalinity pumped. Previous work that examined alkalinity addition in different coarse latitude bands²² found not all areas are equally efficient at CO_2 uptake or retention. We extend this work with a finegrained map and find that on short timescales the efficiency is dominated by the local surface efficiency and atmospheric $p\text{CO}_2$. However, after some time surface currents spread the excess surface alkalinity and the effect becomes less pronounced. For the case of alkalinity addition (rather than pumping) most of the locations eventually reach close to the full average efficiency of 0.85 except areas of significant downwelling in the polar regions (see Fig. S3, ESI†). The alkalinity is pulled downwards and removed from the surface as is evident in depth plots of calcite saturation (Fig. S5, ESI†). In the case of acidity pumping the behaviour is very similar, but on longer timescales, uptake efficiency becomes dominated by the rate of acid return. Since deep return currents

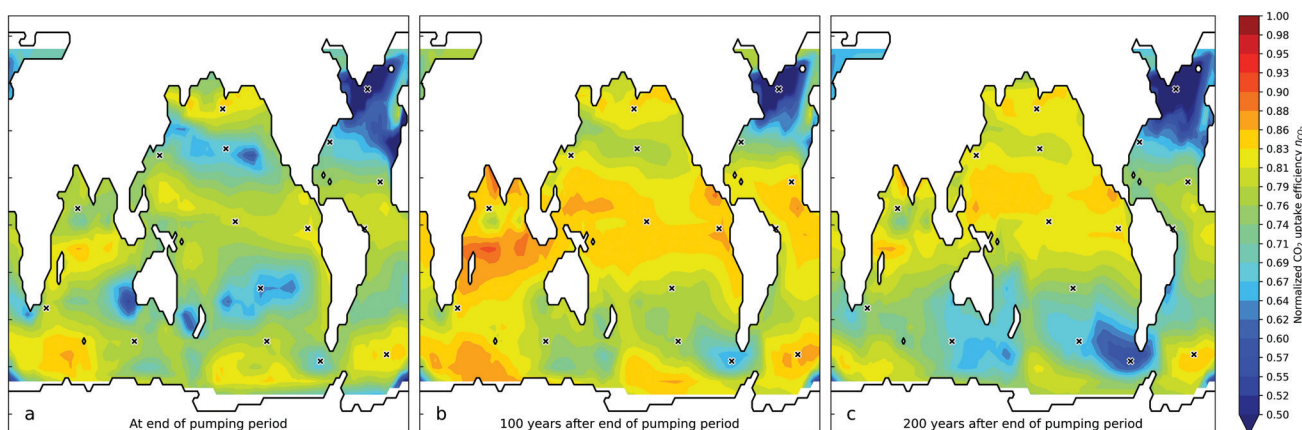


Fig. 5 Efficiency of alkalinity pumping (η_{CO_2}) as a function of latitude and longitude. Here (η_{CO_2}) is the number of moles of excess CO_2 absorbed by the ocean normalized by the number of moles of alkalinity pumped. Each point on the grid represents an entire ocean simulation in which 1 Tmol per year were pumped at that point only (a total of ~ 1000 simulations). Mapped is the relative increase in total oceanic dissolved inorganic carbon (relative to the reference), normalized by the amount of acidity pumped. Three different timepoints are shown: (a) uptake of CO_2 at the end of the 50 year pumping period. Significant differences in the effective η_{CO_2} are observed, depending on where the alkalinity was pumped, varying from 0.5 to 0.85. The differences during this period are driven primarily by the efficiency of CO_2 uptake, as the distribution closely matches that of simple alkalinity addition (cf. Fig. S6, ESI†). In particular the northern Atlantic exhibits poor CO_2 uptake. (b) CO_2 uptake 100 years after the end of pumping. Alkalinity pumping in most northern hemisphere areas has caught up to an uptake efficiency of 0.85 with equatorial regions exhibiting the best retention. (c) 200 years after the end of pumping. The apparent CO_2 uptake is fully dominated by the acid return kinetics (cf. Fig. S6 (ESI†), where alkalinity was added instead of pumped). It is apparent that acidity pumping in the southern hemisphere is less efficient, likely due to the fact that ventilation of deep water occurs in the Southern Ocean and thus acidity returns to the surface more rapidly. Conversely the North Pacific retains pumped acidity the best.



generally move southwards, injection of acidity in the northern hemisphere appears to be significantly more efficient in the long run, with some small areas as notable exceptions. Two large areas in the southern ocean appear to return acidity faster than others and are inefficient locations for alkalinity pumping (Fig. 5). Fig. S3 (ESI†) gives detailed plots of the total excess absorbed CO₂ due to pumping at a selected number of locations. We compared our computed CO₂ retention times with results from a multi-model comparison⁴⁸ which used models of comparable resolution to simulate direct CO₂ injection (see Fig. S7, ESI†). We find, in general, good agreement for almost all locations and depths with the model ensemble.

3.3 Impact on surface and deep water pH

Understanding the pH sensitivity of different locations allows optimization of the alkalization strategy to minimize ecological effects and costs while maximizing CO₂ uptake.

At the surface, the pH increase will be highest right at the injection site, decreasing exponentially with distance. The alkalinity will be compensated by CO₂ uptake, but depending on the local currents and eddies which transport and distribute the alkalinity, as well as wind speeds, surface agitation and local atmospheric CO₂ concentration, we can expect different sensitivities at different injection sites. It is important to avoid too large a pH change both for ecological reasons as well as needing to avoid triggering inorganic precipitation⁴⁹ of CaCO₃. At depth, the injection of acidity must also be considered against an ecological safety margin. We propose that the acidity is injected no closer than 500 m to the seafloor and at least 2000 m from the surface. This area of the ocean is the least

populated by marine species and thus gives ample time for the acidity to dilute horizontally away from the diffuser pipes. Fig. 6 shows the sensitivity of surface and deep water pH on the pumping location from ~1000 individual simulations of single-point alkalinity pumping. The sensitivity (m² s mol⁻¹) was calculated by dividing the maximal ΔpH observed for any given simulation by the pumping rate density (mol m⁻² s⁻¹). As expected, areas with stronger surface currents spread surface alkalinity most efficiently, reducing the pH impact at the release location. This effect would be less pronounced if the release stations were free floating with these bulk water movements; however, the horizontal eddy diffusivity is considerably larger in these currents, which would make them preferential release sites nevertheless. Another factor reducing surface pH impact are wind speeds, which reduce the ocean-atmosphere CO₂ equilibration time. The circumpolar wind band likely accounts for the low surface sensitivities observed in the southern ocean (Fig. 6 and Fig. S4, ESI†).

4 Discussion

4.1 Deployment possibilities

The proposed method is only reliant on local resources (seawater) and power and could be implemented in a variety of locations with varying power sources, as shown in Fig. 1. Specifically, it would be uniquely matched for untethered power generators, obviating the otherwise arising problem of energy storage or transmission and material transport encountered in other offshore methods,⁵⁰ thus providing a productive use of open-ocean power sources *in situ*.

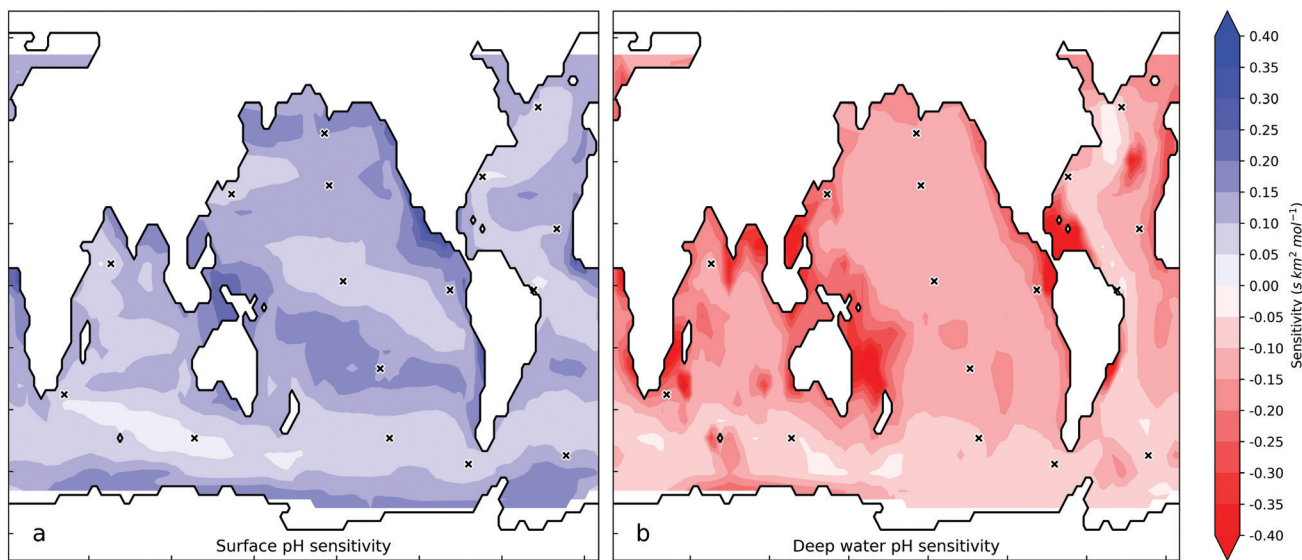


Fig. 6 Local surface pH sensitivity in s km² mol⁻¹ obtained by injection at each grid point only (each grid point represents an entire independent simulation). The sensitivity was calculated by dividing the globally maximal ΔpH in either direction observed for any given simulation by the pumping rate density (mol km⁻² s⁻¹). Panel (a) reflects pH changes in the alkaline direction (typically found at the surface release site). The surface sensitivity represents the efficiency with which a stationary addition of alkalinity at any given location with some constant rate is distributed and neutralized by CO₂ invasion. Larger values indicate slower spreading from the release site and/or slower neutralization by CO₂ invasion. Areas with stronger surface currents can spread surface alkalinity most efficiently and are least sensitive to surface pH changes. Panel (b) reflects pH changes in the acidic direction (found in deep water where the acidity is pumped to). The crosses mark the location of the individual plots in Fig. S4 (ESI†).



Open-ocean stations could operate on wave, wind or ocean thermal (OTEC^{51–54}) power and could be scaled with a large number of untethered, identical units. Open-ocean photovoltaics have been investigated⁵⁵ and trial projects are underway.⁵⁶ All of these technologies are still in early development and have not yet benefited from commercial efficiencies of scale and are thus currently relatively expensive. Part of the reason for the lack of wide scale adoption is the need for energy transmission in one form or another. Ocean acidity pumping could thus be a perfect match for these technologies. The lack of need for power transmission or transport can further reduce costs compared to current estimates. Alkalinity release in open waters, rather than coastal waters, might be less impactful to marine biology permitting deployment at larger scale.

An alternative approach could involve near-coast operation; larger sized plants could tap into cheap terrestrial energy, especially daytime excess solar. Acid/base generators could potentially be located just-off-coast with a grid connection to land – transportation of electricity being considerably cheaper than transport of matter, *i.e.* the pumping of seawater onto land and back should be avoided.⁵⁷ Decommissioned oil rigs may offer an ideal platform for such deployment.

Coastal locations where the continental slope is close to the coast and strong surface currents occur would be preferred, because they shorten the distance acid and base need to be transported, and currents would be able to distribute the excess surface alkalinity effectively. A potential intermediate deployment would consist of near-shore wind farms. Where possible, especially in areas where deep waters are not accessible, the acid stream could also be injected underground, into basalt formations^{58–60} or depleted oil wells where it would react with silicate rocks and be neutralized.¹⁶ Injection of hydrochloric acid into rock formations is conceptually similar to the CarbFix process⁵⁸ and more generally to carbon capture and storage approaches (CCS).⁶¹ However experimental studies of injectivity, the ensuing *in situ* chemistry and the storage capacities for such acid injections are needed to assess the viability of this approach. Injection into depleted oil reservoirs might be appropriate for example for the North Sea although such areas may be limited to smaller amounts of alkalinity that can be safely released while keeping pH changes below ecological thresholds. However, this could present a feasible method to stabilize ocean pH in localized areas to counteract ecological damage from acidification.^{18–20}

4.2 Techno-economic estimation

Although a full techno-economic analysis is beyond the scope of this paper, we conduct a rough estimation of potential costs of electrodialysing seawater using published data from other methods which create pH gradients. Acid/base production could be implemented using either electrolysis or bipolar membrane electrodialysis. Electrolysis was among the first methods suggested for negative emissions technology,¹⁶ though the generation of gases is energetically inefficient and has to be either recouped using a fuel cell, adding complexity and cost, or recouped by selling the products,²⁸ which

necessitates mass transport of the products.⁵⁰ The use of electrolysis on seawater at gigatonne scale may also produce significant quantities of volatile halogenated organics which are ozone depleting, such as bromo- and chloromethane.¹⁷ Here we choose to focus on electrodialysis methods, which have been proposed and tested for seawater CO₂ extraction.^{62–67} However, even if colocated with desalination plants, costs are high (373–604\$ per tCO₂,⁶³ 540\$ per tCO₂⁶⁶) in part due to very large quantities of seawater needing to be processed (about 11 000 m³ tCO₂⁻¹). In contrast, releasing the alkalinity to the ocean for passive CO₂ absorption and storage is conceptually and technologically simpler, consisting only of the acid/base generator. The quantity of seawater needing to be processed is greatly reduced (100–500 m³ tCO₂⁻¹ depending on the exact concentration of effluent acid and base). There is no CO₂ extraction, thus saving capital and operational costs of membrane contactors⁶³. Indeed Digdaya *et al.* found membrane contactors and vacuum pumps accounted for 90% of the equipment cost.⁶⁶ Instead, leveraging the ocean as a sorbent surface obviates the need for air contactors as well as additional storage, as the CO₂ is stored as relatively benign bicarbonate ions. From a capital and operational cost perspective, alkalinity pumping is a strict subset of electrodialysis-driven CO₂ extraction and should thus always be cheaper, whether the acidity is moved to deep ocean or underground. The three largest contributors to overall leveled cost would be the cost of electricity to drive the electrodialysis stack, the cost of pre-treating seawater to prevent fouling of the membrane stack and the cost and lifetime of the membranes themselves. Minor contribution costs are the pumping of acidified water to depth. In the open ocean scenario we assume that the cost of the structure are implicit in the assumed leveled costs for open-ocean electricity, and that the electrodialysis apparatus is generally much smaller than the structure. In the following we discuss the likely current ranges of these costs and likely learning curve improvements into the future. However it should be noted that in order to further narrow these estimates, construction of medium-size prototypes⁶³ is essential.

4.2.1 Energy costs. In bipolar membrane electrodialysis (BPMED), the thermodynamic minimum energy to create effluent streams at a given pH can be calculated from the Nernst equation as

$$\Delta G = 2.303RT\Delta\text{pH} \quad (4)$$

where ΔpH is the pH difference between the acid and base effluents. For a base effluent concentration of 1 M NaOH, the minimum energy is ~ 80 kJ mol⁻¹ ($E^0 \approx 0.83$ V) at ambient conditions. A real BPMED stack of course will require considerably more energy due to ohmic losses in the membranes and the thin solution layers, electrolytic losses at the electrodes, and back-leakage of protons or hydroxide ions. Electrodialysis is, in principle, more efficient than electrolysis for creating a pH gradient, since no additional energy is expended to generate gaseous O₂ or H₂ ($E^0 = 1.23$ V) which has to be recouped economically⁵⁰ or *via* fuelcell.¹⁶ The specific energy consumption (E_{sp} , kJ mol⁻¹) varies substantially in the literature ranging from 160 to over 350 kJ mol⁻¹



(162 kJ mol⁻¹⁶⁸ 155 kJ mol⁻¹⁶⁶ 242 kJ mol⁻¹⁶³ 236 kJ mol⁻¹⁶⁷ 255 kJ mol⁻¹⁶⁹ 259 kJ mol⁻¹⁷⁰ 328 kJ mol⁻¹⁷¹ 341 kJ mol⁻¹⁷²). This represents process efficiencies of only 20–45%, suggesting that there is potential for learning curves and technological improvements. Many of the above studies aim to valorize reject brines and are optimized to produce both concentrated (>1 M) and pure acids and bases for industrial use and thus require deionized water to feed acid and base tanks in feed-and-bleed flow schemes. For purposes of acidity pumping the effluent can be more impure and dilute than in the above studies, affording potentially lower costs. The leveled cost of electricity for free floating power generation is highly variable, and likely suboptimal due to the lack of current economies. Wind power has been estimated at \$30–80 per MWh.⁵⁴ OTEC is estimated to provide energy at a cost of \$150–200 per MWh.^{50,53} Wave power generators leveled costs are highly uncertain and maybe in the range of \$120–470 per MWh.⁷³ Even though transmission costs can be saved in our case, the present-day costs are likely too high for economical carbon capture, but have considerable potential for reduction with economies of scale. As an alternative, land-base power could be used in near-coast applications where strong currents allow for nearby alkalinity distribution. Examples include the Agulhas, the Kuroshio, the Gulfstream and the North Brazilian current. However deep-water acid disposal becomes more limited as bottom currents are much slower and it may be better to instead pump the acidified stream underground if suitable underground formations are available. Utility scale solar is likely the cheapest land-based energy source with unsubsidized leveled costs as cheap as \$32–44 per MWh and wind at \$28–54 per MWh.⁷⁴ It is thought that there will be a considerable excess of this power during daytime hours, for which finding a carbon negative use would be desirable to help with load leveling.

Assuming an efficiency range of 160–250 kJ mol⁻¹, energy prices of \$30–80 per MWh and an ocean uptake efficiency η_{CO_2} of 0.8 we obtain a range for the energy costs of \$38–158 per tCO₂. It is interesting to compare these energy requirements to other CDR approaches. Electrolytic approaches require about ~300 kJ mol⁻¹.²⁸ Direct air capture (DAC) had been estimated at 312–524 kJ mol⁻¹.⁷⁵ A comprehensive analysis of recent DAC methods reported 371–546 kJ mol⁻¹ for liquid solvent approaches and 174–260 kJ mol⁻¹ for solid sorbents,⁷⁶ however much of the energy required is heat rather than electrical.

Energy requirements for methods involving mafic or ultramafic rocks to the ocean, likely needing to be ground to 1 µm for open ocean application,²² vary substantially from^{15,49} 175–315 kWh t⁻¹ to²⁴ 500–1000 kWh t⁻¹. Depending on the rock type, with a net uptake efficiency of 0.3–0.8 tCO₂ per tonne of rock, one obtains an energy requirement of 35–528 kJ per mol of CO₂ absorbed.

4.2.2 Water pretreatment costs. As ion-exchange membranes are prone to scaling and fouling,⁷⁷ methods that electrodialyse seawater typically use nano-filtration (nF) and reverse osmosis (RO) pretreatment to remove divalent ions,^{62,70} concentrate the input brine and provide deionized water, especially for the base compartment where scaling would be most pronounced. The associated costs are not negligible and

tradeoffs need to be considered. Higher flow rates increase pretreatment costs but reduce concentration gradients in the BPMED stack leading to higher faradaic efficiency. There is a tradeoff point, typically around 0.5–1.0 M effluent acid/base, corresponding to a pretreated water need of 56–114 m³ tCO₂⁻¹ (accounting for an uptake factor of 0.8). We estimate the cost of water pretreatment⁷⁸ at \$0.5 per m³, leading to a cost range of \$28–57 per tCO₂. Development of BPMED processes which are more resistant to fouling, may mitigate this pretreatment cost.

4.2.3 Bipolar membrane capital costs. Current densities in BPM stacks vary typically between 450–700 A m⁻¹ and cell resistivities of ~0.003 Ω m³, giving a power density of $P_D = 1.5\text{--}0.6 \text{ kW m}^{-2}$. We can thus calculate the leveled cost contribution of the membranes as $C_M \eta E_{\text{sp}} / P_D$, where C_M (\$s⁻¹ m⁻²) is the leveled discounted cost of the membranes and $\eta = 0.8$ is the CO₂ uptake efficiency. Lower current densities improve the energy efficiency due to lower resistive losses but increase membrane capital costs,⁷¹ leading to cost tradeoffs. Reduction of membrane costs by 5–10× through economies of scale and technological advances⁷⁹ thus has the opportunity to drastically reduce energy costs. Commercial bipolar membrane stacks (consisting of one bipolar membrane and two monopolar membranes) are currently produced at relatively small quantities, but at moderate scale, with an assumed active lifetime of about 3 years, we could reasonably expect a leveled cost^{63,66} of $C_M = \$200 \text{ year}^{-1} \text{ m}^{-2}$. Thus we estimate the membrane capital cost contribution between \$20–75 per tCO₂.

4.2.4 Dispersion. Depending on the deployment mode, the alkalinity and acidity need to be separated and transported. In the case of open ocean deployment, the alkalinity is simply released on site, while the acidity is pumped to depth. We can assume that the capital costs of the floating structure are implicitly included in the leveled cost of the chosen offshore energy system, as the electrodialysis unit would be quite small compared to the energy structure. We can estimate the additional requirements for pumping as follows. Assuming an acid concentration of 0.5–1.0 M, the quantity of water to be pumped is 28–56 m³ tCO₂⁻¹. As no net work is done against gravity, the energy for pumping is that of overcoming the friction in the pipe. We can estimate the head loss (in meters of water) using the empirical Hazen–Williams equation (in SI units):

$$h_f = 10.67 \left(\frac{Q}{C} \right)^{1.852} d^{-4.8704} L \quad (5)$$

where Q is the flow rate (m³ s⁻¹), d and L are the diameter and length of the pipe (m), respectively, and C is an empirical pipe roughness coefficient, about 140 for a typical smooth pipe. For example a 3000 m long pipe, 5 cm wide, and a flow rate of 5 L s⁻¹ would require a head pressure of ~40 bar. This is quite similar to injection of CO₂ into basalt formations requiring ~27 m³ tCO₂⁻¹ of water and pressures of 25 bar.⁵⁸ The power needed to pump water at a rate of Q through the pipe is given by:

$$P_{\text{pump}} = h_f' w Q \quad (6)$$

where γ_w is the specific weight of water, 9.8 kN m^{-3} . The power required to generate the acid and base is given by

$$P_{ED} = c_H E_{sp} Q \quad (7)$$

where E_{sp} is the specific energy requirement of the BPMED stack (kJ mol^{-1}) and c_H is the concentration of acid produced ($c_H = 10^{-\text{pH}}$). Assuming for example $c_H \approx 0.75 \text{ M}$ and $E_{sp} \approx 180 \text{ kJ mol}^{-1}$ we obtain $P_{ED} \approx 675 \text{ kW}$ and $P_{\text{pump}} \approx 20 \text{ kW}$, just 3% of the dialysis energy requirements. However, the engineering requirements for a deep-ocean pipe system are non-negligible, resembling in many ways that of deep ocean lift cables for deep ocean ROV systems in terms of size, design and required resistance to ocean stress. The amortized costs, for a production at scale, are highly dependent on the particular ocean location and mode of deployment and thus difficult to estimate. As an orientation, if we assume conservatively a 5 year lifespan and a cost of \$60 per m for a 2500 m pipe we obtain a leveled cost of about \$7.2 per tCO_2 . However the challenges of open-sea engineering are formidable and pilot studies would be necessary to narrow the cost estimates.

If alkalinity is generated near shore at scale it will need to be dispersed away far from the shore to avoid local pH spikes. However, because the alkalinity is relatively dilute ($0.1\text{--}1 \text{ mol kg}^{-1}$) compared to dry solid alkaline materials ($\sim 25 \text{ mol kg}^{-1}$) bulk transportation is considerably less efficient. For example, at $\eta = 0.8$, 28.4 tonnes of 1 mol kg^{-1} hydroxide solution are required for every tonne of CO_2 absorbed. Large-scale maritime shipping costs are around \$0.0016–0.004 per t per km and produce about 7 gCO_2 per t per km.⁴⁹ Assuming alkalinity to be dispersed in a 150 km strip around the coast, *i.e.* well within the exclusive economic zone of any bordering country, and typical tanker speeds of 14 knots (7.2 m s^{-1}), the 300 km roundtrip (150 km zone) could be completed in 12 hours, with a daily turnaround. Assuming a factor of 2 inefficiency compared to ordinary shipping, due to the very frequent loading, we obtain a cost of \$13–33 per tCO_2 . Furthermore, as tankers are hard to decarbonize, $\sim 57 \text{ kgCO}_2$ are emitted for every tonne of CO_2 absorbed, about a 5% reduction in efficiency. The additional costs and the additional CO_2 impact of transport limit alkalinity release to coastal areas and thus limit the total scaling of land-based alkalinity production.

Overall for open-ocean deployment we obtain a minimum cost per tonne of CO_2 captured of $\sim \$93\text{--}297$ per tCO_2 . This estimate is quite close to estimations obtained by a recent study^{57,63} ($110\text{--}325\text{\$}$ per tCO_2) for the BPMED portion of their process, which conducted a much more detailed technoeconomic analysis for CO_2 extraction. As expected the costs are much lower than estimates for CO_2 extraction ($373\text{--}604\text{\$}$ per tCO_2 ⁶³, $540\text{\$}$ per tCO_2 ⁶⁶)

At the lower end, the total cost estimate has similar-sized cost contributions from energy cost, membrane cost and water treatment cost. Thus to drive down overall costs development and cost reduction is needed in all three areas. We note that the dialysis membrane industry is currently very small and very significant cost savings could be expected at scale.⁷⁹ Furthermore, as with all ocean CDRs, working with ocean water and in marine environments in general poses significant challenges in terms of

corrosion and longevity of the equipment which will need to be addressed for a practical, scalable application.

For comparison, costs for direct air capture have been reported at \$89–407 per tCO_2 for solid sorbent systems and \$156–506 per tCO_2 for liquid solvent systems.⁷⁶ The operational costs of enhanced weathering has been estimated at \$70–578 per tCO_2 and \$24–123 per tCO_2 for basic and ultrabasic rocks respectively⁴⁹ and ocean liming falls in the \$72–159 per tCO_2 range.¹³

5 Conclusions

We have explored the feasibility of accelerating the natural compensation of ocean acidification by CaCO_3 deposits by artificially pumping excess acidity towards the abyssal CaCO_3 sediments. The subsequent alkalinization of the surface would counteract anthropogenic acidification and increase the uptake of significant quantities of atmospheric CO_2 . Thus alkalinity pumping could meaningfully contribute to a portfolio of negative emissions technologies. Based on our simulation we estimate 1–3 GtC per year could be removed over a 50 year period, without lowering deep water pH by more than 0.2. For acid injection depth $> 3000 \text{ m}$ we show that carbonate compensation is significantly engaged, permanently removing up to 40% of the absorbed CO_2 . Reemission of the remainder occurs only after 300 years and slowly over several millennia of gradual outgassing, effectively flattening the curve of the anthropogenic CO_2 shock to the atmosphere. In theory up to 150 GtC could be removed this way before the end of the century, satisfying requirements for negative emissions laid out by RCP2.6 pathways. What might a scaled up deployment look like? Modern offshore 10 MW wind turbines can generate on the order of 50 GWh of energy per year, which could be used to sequester on the order of 10 ktC per year. Thus for a total scale of 1 GtC per year about 100 000 of such units would be necessary (*i.e.* about 1000 GW of total capacity). For comparison current global offshore wind capacity is already expected to reach about 500 GW by 2050, thus a goal of 1 GtC per year negative emissions could be feasible before the end of the century.

The pumping of ocean acidity presented in this paper avoids many of the environmental issues with mineral-adding alkalinity methods both in terms of impurity dissolution in the ocean and mining impacts on land. It is conceptually simple and requires only locally available resources (seawater and energy), and is thus uniquely suited to openwater deployment. While in the short term, on-shore electrochemical alkalinization is likely more economical due to the inherent engineering challenges of marine engineering, it is also inherently limited in scale. We have shown that transport of dilute acid or base is not economical beyond 150 km away from the production site. Disposal of dilute acid into deep basalt aquifers provides a partial solution but its scaling limits are not well understood. Therefore open-water production of acid and base could supplement terrestrially powered CDR and is an interesting



avenue of research despite the usual challenges of marine engineering. Open-water CDR also provides a route to make use of otherwise unusable renewable energy, an area of CDR research that has been underexplored. In general, manipulation of acidity/alkalinity as a proxy for CO₂ may be technologically simpler and/or more efficient than manipulation of CO₂ directly, whether the acidity is moved into deep ocean or underground. We also presented a fine-grained analysis of location dependence of surface alkalization and show that in the short term there is substantial variation in CO₂ uptake efficiency which will need to be considered in any ocean alkalization plan, mineral-based or not. As with all ocean-based CDR methods, simulations have inherent limits and the ecological parameters and limitations require substantial further research of natural analogues⁴⁵ and experimentation in meso-scale pilot programs.

Conflicts of interest

There are no conflicts to declare.

Acknowledgements

We thank Matt Eisaman, Ben Saenz, Rob Dunbar, Joel Atwater, Will Regan, Eli Patten, Daniel Rosenfeld and Kevin McCloskey for many helpful discussions and comments on the manuscript.

Notes and references

- 1 S. J. Davis, N. S. Lewis, M. Shaner, S. Aggarwal, D. Arent, I. L. Azevedo, S. M. Benson, T. Bradley, J. Brouwer, Y.-M. Chiang, C. T. M. Clack, A. Cohen, S. Doig, J. Edmonds, P. Fennell, C. B. Field, B. Hannegan, B.-M. Hodge, M. I. Hoffert, E. Ingersoll, P. Jaramillo, K. S. Lackner, K. J. Mach, M. Mastrandrea, J. Ogden, P. F. Peterson, D. L. Sanchez, D. Sperling, J. Stagner, J. E. Trancik, C.-J. Yang and K. Caldeira, *Science*, 2018, **360**, eaas9793.
- 2 L. T. Bach, S. J. Gill, R. E. M. Rickaby, S. Gore and P. Renforth, *Front. Clim.*, 2019, **1**, 7.
- 3 G. P. Peters, *Nat. Clim. Change*, 2016, **6**, 646–649.
- 4 J. E. Dore, R. Lukas, D. W. Sadler, M. J. Church and D. M. Karl, *Proc. Natl. Acad. Sci. U. S. A.*, 2009, **106**, 12235–12240.
- 5 D. Archer, M. Eby, V. Brovkin, A. Ridgwell, L. Cao, U. Mikolajewicz, K. Caldeira, K. Matsumoto, G. Munhoven, A. Montenegro and K. Tokos, *Annu. Rev. Earth Planet. Sci.*, 2009, **37**, 117–134.
- 6 D. Archer, H. Kheshgi and E. Maier-Reimer, *Geophys. Res. Lett.*, 1997, **24**, 405–408.
- 7 D. Archer, H. Kheshgi and E. Maier-Reimer, *Global Biogeochem. Cycles*, 1998, **12**, 259–276.
- 8 D. Archer, *J. Geophys. Res.*, 2005, **110**, C9.
- 9 N. S. Lord, A. Ridgwell, M. C. Thorne and D. J. Lunt, *Global Biogeochem. Cycles*, 2016, **30**, 2–17.
- 10 J. L. Sarmiento and N. Gruber, *Ocean biogeochemical dynamics*, Princeton University Press, Princeton, 2006.
- 11 O. Sulpis, B. P. Boudreau, A. Mucci, C. Jenkins, D. S. Trossman, B. K. Arbic and R. M. Key, *Proc. Natl. Acad. Sci. U. S. A.*, 2018, **115**, 11700–11705.
- 12 L.-Q. Jiang, B. R. Carter, R. A. Feely, S. K. Lauvset and A. Olsen, *Sci. Rep.*, 2019, **9**, 18624.
- 13 P. Renforth and G. Henderson, *Rev. Geophys.*, 2017, **55**, 636–674.
- 14 F. Montserrat, P. Renforth, J. Hartmann, M. Leermakers, P. Knops and F. J. R. Meysman, *Environ. Sci. Technol.*, 2017, **51**, 3960–3972.
- 15 S. J. Hangx and C. J. Spiers, *Int. J. Greenhouse Gas Control*, 2009, **3**, 757–767.
- 16 K. Z. House, C. H. House, D. P. Schrag and M. J. Aziz, *Environ. Sci. Technol.*, 2007, **41**, 8464–8470.
- 17 G. H. Rau, S. A. Carroll, W. L. Bourcier, M. J. Singleton, M. M. Smith and R. D. Aines, *Proc. Natl. Acad. Sci. U. S. A.*, 2013, **110**, 10095–10100.
- 18 M. Mongin, M. E. Baird, A. Lenton, C. Neill and J. Akl, *Environ. Res. Lett.*, 2021, **16**, 064068.
- 19 R. Albright, L. Caldeira, J. Hosfelt, L. Kwiatkowski, J. K. Maclare, B. M. Mason, Y. Nebuchina, A. Ninokawa, J. Pongratz and K. L. Ricke, *et al.*, *Nature*, 2016, **531**, 362–365.
- 20 E. Y. Feng, D. P. Keller, W. Koeve and A. Oschlies, *Environ. Res. Lett.*, 2016, **11**, 074008.
- 21 P. Ziveri, B. de Bernardi, K.-H. Baumann, H. M. Stoll and P. G. Mortyn, *Deep Sea Res., Part II*, 2007, **54**, 659–675.
- 22 P. Köhler, J. F. Abrams, C. Völker, J. Hauck and D. A. Wolf-Gladrow, *Environ. Res. Lett.*, 2013, **8**, 014009.
- 23 *Project Vesta*, <https://www.projectvesta.org/>.
- 24 J. J. Li and M. Hitch, *Int. J. Min., Metall. Mater.*, 2015, **22**, 1005–1016.
- 25 D. J. Beerling, J. R. Leake, S. P. Long, J. D. Scholes, J. Ton, P. N. Nelson, M. Bird, E. Kantzas, L. L. Taylor and B. Sarkar, *et al.*, *Nat. Plants*, 2018, **4**, 138–147.
- 26 T. Simkin and J. V. Smith, *J. Geol.*, 1970, **78**, 304–325.
- 27 J. B. Glass and C. L. Dupont, *Oceanic Nickel Biogeochemistry and the Evolution of Nickel Use*, Royal Society of Chemistry, 2019, ch. 2, pp. 12–26.
- 28 G. H. Rau, H. D. Willauer and Z. J. Ren, *Nat. Clim. Change*, 2018, **8**, 621–625.
- 29 *Convention on the Prevention of Marine Pollution by Dumping of Wastes and Other Matter*, 1972.
- 30 R. M. Webb, K. Silverman-Roati and M. B. Gerrard, Removing Carbon Dioxide Through Ocean Alkalinity Enhancement: Legal Challenges and Opportunities, <https://climate.law.columbia.edu/sites/default/files/content/Webb>.
- 31 *IPCC special report on carbon dioxide capture and storage*, ed. B. Metz and Intergovernmental Panel on Climate Change, Cambridge University Press, for the Intergovernmental Panel on Climate Change, Cambridge, 2005.
- 32 P. W. Boyd, A. J. Watson, C. S. Law, E. R. Abraham, T. Trull, R. Murdoch, D. C. E. Bakker, A. R. Bowie, K. O. Buesseler, H. Chang, M. Charette, P. Croat, K. Downing, R. Frew, M. Gall, M. Hadfield, J. Hall, M. Harvey, G. Jameson, J. LaRoche, M. Liddicoat, R. Ling, M. T. Maldonado, R. M. McKay, S. Nodder, S. Pickmere, R. Pridmore,



S. Rintoul, K. Safi, P. Sutton, R. Strzepek, K. Tanneberger, S. Turner, A. Waite and J. Zeldis, *Nature*, 2000, **407**, 695–702.

33 S. A. Rackley, *Carbon Capture and Storage*, Elsevier, 2010, pp. 267–286.

34 *Massachusetts Institute of Technology General Circulation Model*, <https://mitgcm.org/>.

35 S. Dutkiewicz, A. Sokolov, J. Scott and P. Stone, *A three-dimensional ocean-seaice-carbon cycle model and its coupling to a two dimensional atmospheric model: Uses in climate change studies. Report 122, MIT Joint Program on the Science and Policy of Global Change*, 2005, http://mit.edu/global-change/www/MITJPSPGC_Rpt122.pdf [Online; accessed 20-April-2021].

36 A. Lenton, R. J. Matear, D. P. Keller, V. Scott and N. E. Vaughan, *Earth Syst. Dynam.*, 2018, **9**, 339–357.

37 M. F. González and T. Ilyina, *Geophys. Res. Lett.*, 2016, **43**, 6493–6502.

38 J. J. Middelburg, K. Soetaert and M. Hagens, *Rev. Geophys.*, 2020, **58**, e2019RG000681.

39 W. M. Berelson, W. M. Balch, R. Najjar, R. A. Feely, C. Sabine and K. Lee, *Global Biogeochem. Cycles*, 2007, **21**, GB1024.

40 B. P. Boudreau, J. J. Middelburg and F. J. R. Meysman, *Geophys. Res. Lett.*, 2010, **37**, L03603.

41 B. P. Boudreau, *Geophys. Res. Lett.*, 2013, **40**, 744–748.

42 Download: https://gresearch.storage.googleapis.com/climate-energy/acidity/CO2_Capture_by_pumping_acidity.tgz.

43 M. Hagens and J. J. Middelburg, *Geophys. Res. Lett.*, 2016, **43**, 12528–12537.

44 C. E. Cornwall, C. D. Hepburn, C. M. McGraw, K. I. Currie, C. A. Pilditch, K. A. Hunter, P. W. Boyd and C. L. Hurd, *Proc. R. Soc. B*, 2013, **280**, 20132201.

45 L. T. Bach and P. W. Boyd, *Seeking natural analogs to fast-forward the assessment of marine CO₂ removal*, 2021, DOI: 10.1073/pnas.2106147118.

46 M. P. Humphreys, L. Gregor, D. Pierrot, S. M. A. C. van Heuven, E. R. Lewis and D. W. R. Wallace, *PyCO2SYS: marine carbonate system calculations in Python*, 2020, <https://zenodo.org/record/3744275>.

47 E. R. Lewis and D. W. R. Wallace, *Program Developed for CO₂ System Calculations*, 1998.

48 J. C. Orr, O. Aumont, A. Yool, K. Plattner, F. Joos, E. Maier-Reimer, M.-F. Weirig, R. Schlitzer, K. Caldeira, M. E. Wickett and R. J. Matear, *Ocean CO₂ sequestration efficiency from 3-d ocean model comparison*, 2001.

49 P. Renforth, *Int. J. Greenhouse Gas Control*, 2012, **10**, 229–243.

50 G. H. Rau and J. R. Baird, *Renewable Sustainable Energy Rev.*, 2018, **95**, 265–272.

51 J. R. Chiles, *The Other Renewable Energy*, 2009, <https://www.inventionandtech.com/content/other-renewable-energy-0> [Online; accessed 20-April-2021].

52 F. Kreith and D. Bharathan, *J. Heat Transfer*, 1988, **110**, 5–22.

53 L. Liu, *New J. Phys.*, 2014, **16**, 123019.

54 A. Babarit, J.-C. Gilloteaux, G. Clodic, M. Duchet, A. Simoneau and M. F. Platzer, *Int. J. Hydrogen Energy*, 2018, **43**, 7266–7289.

55 S. Z. Golroodbari and W. Sark, *Prog. Photovoltaics*, 2020, **28**, 873–886.

56 B. Willis, *The Race Is On for Commercial Deployment of Solar in Open Seas*, 2021, <https://www.greentechmedia.com/articles/read/race-on-for-commercial-deployment-of-solar-in-open-seas> [Online; accessed 20-April-2021].

57 M. D. Eisaman, *Joule*, 2020, **4**, 516–520.

58 J. M. Matter, W. Broecker, M. Stute, S. Gislason, E. Oelkers, A. Stefánsson, D. Wolff-Boenisch, E. Gunnlaugsson, G. Axelsson and G. Björnsson, *Energy Procedia*, 2009, **1**, 3641–3646.

59 B. P. McGrail, H. T. Schaef, A. M. Ho, Y.-J. Chien, J. J. Dooley and C. L. Davidson, *J. Geophys. Res.*, 2006, **111**, B12201.

60 D. S. Goldberg, T. Takahashi and A. L. Slagle, *Proc. Natl. Acad. Sci. U. S. A.*, 2008, **105**, 9920–9925.

61 M. Bui, C. S. Adjiman, A. Bardow, E. J. Anthony, A. Boston, S. Brown, P. S. Fennell, S. Fuss, A. Galindo, L. A. Hackett, J. P. Hallett, H. J. Herzog, G. Jackson, J. Kemper, S. Krevor, G. C. Maitland, M. Matuszewski, I. S. Metcalfe, C. Petit, G. Puxty, J. Reimer, D. M. Reiner, E. S. Rubin, S. A. Scott, N. Shah, B. Smit, J. P. M. Trusler, P. Webley, J. Wilcox and N. Mac Dowell, *Energy Environ. Sci.*, 2018, **11**, 1062–1176.

62 M. D. Eisaman, J. L. Rivest, S. D. Karnitz, C.-F. de Lannoy, A. Jose, R. W. DeVaul and K. Hannun, *Int. J. Greenhouse Gas Control*, 2018, **70**, 254–261.

63 C.-F. de Lannoy, M. D. Eisaman, A. Jose, S. D. Karnitz, R. W. DeVaul, K. Hannun and J. L. Rivest, *Int. J. Greenhouse Gas Control*, 2018, **70**, 243–253.

64 H. D. Willauer, F. DiMascio, D. R. Hardy and F. W. Williams, *Energy Fuels*, 2017, **31**, 1723–1730.

65 B. D. Patterson, F. Mo, A. Borgschulte, M. Hillestad, F. Joos, T. Kristiansen, S. Sunde and J. A. van Bokhoven, *Proc. Natl. Acad. Sci. U. S. A.*, 2019, **116**, 12212–12219.

66 I. A. Digdaya, I. Sullivan, M. Lin, L. Han, W.-H. Cheng, H. A. Atwater and C. Xiang, *Nat. Commun.*, 2020, **11**, 362–365.

67 F. Sabatino, M. Mehta, A. Grimm, M. Gazzani, F. Gallucci, G. J. Kramer and M. van Sint Annaland, *Ind. Eng. Chem. Res.*, 2020, **59**, 7007–7020.

68 J. R. Davis, Y. Chen, J. C. Baygents and J. Farrell, *ACS Sustainable Chem. Eng.*, 2015, **3**, 2337–2342.

69 J. Farrell and S. Snyder, *Bipolar Membrane Electrodialysis for Zero Liquid Discharge Water Softening and Wastewater Reclamation*, https://west.arizona.edu/sites/default/files/data/3_Research_Jim.

70 M. Reig, S. Casas, C. Valderrama, O. Gibert and J. Cortina, *Desalination*, 2016, **398**, 87–97.

71 Y. Wang, A. Wang, X. Zhang and T. Xu, *Ind. Eng. Chem. Res.*, 2011, **50**, 13911–13921.

72 J. Shen, J. Huang, L. Liu, W. Ye, J. Lin and B. V. der Bruggen, *J. Hazard. Mater.*, 2013, **260**, 660–667.

73 *Annual Report Ocean Energy Systems*, 2015, <https://report2015.ocean-energy-systems.org/> [Online; accessed 20-April-2021].

74 *Lazard's Levelized Cost of Energy Analysis*, 2019, <https://www.lazard.com/media/451086/lazards-levelized-cost-of-energy-version-130-vf.pdf> [Online; accessed 20-April-2021].



75 M. Broehm, J. Strefler and N. Bauer, *Techno-Economic Review of Direct Air Capture Systems for Large Scale Mitigation of Atmospheric CO₂*, 2015, DOI: 10.2139/ssrn.2665702.

76 National Academies of Sciences Engineering and Medicine, *Negative Emissions Technologies and Reliable Sequestration: A Research Agenda*, The National Academies Press, Washington, DC, 2019.

77 M. Hansima, M. Makehelwala, K. Jinadasa, Y. Wei, K. Nanayakkara, A. C. Herath and R. Weerasooriya, *Chemosphere*, 2021, **263**, 127951.

78 A. Alsheghri, S. A. Sharief, S. Rabbani and N. Z. Aitzhan, *Energy Procedia*, 2015, **75**, 319–324.

79 H. Tsuchiya and O. Kobayashi, *Int. J. Hydrogen Energy*, 2004, **29**, 985–990.

